TEAM KMOU MACRO: Design and Competition Strategy for the 2026 Maritime RobotX Challenge

Hongkyun An, Chiung Yun, Changyu Han, Sukhwan Jung,
Wonbin Baek, Donggun Lee, Hyeonjun Lee, JeaYeong Park,
Junyoung Joo, Donghun Kang, Woojoo Jeon, and Joohyun Woo

Korea Maritime & Ocean University

Abstract—Team KMOU MACRO enters the 2026 Maritime RobotX Challenge with a System of Systems (SoS) comprising the Apex unmanned surface vehicle (USV), the Windy unmanned aerial vehicle (UAV), and the Nautilus unmanned underwater vehicle (UUV). Our central design philosophy is that, under a limited testing budget, reliability is won by securing sufficient physical margin and local autonomy in each domain and by bounding the dependencies between vehicles—not by maximizing the number of demonstrable functions. The USV serves as the mission-coordination and communication hub; the UAV and UUV retain onboard perception and control and exchange only mission-level information through the USV, so that a single link or subsystem fault does not propagate across domains. This report links that competition strategy to concrete design decisions—azimuth propulsion for docking, a payload-driven hexacopter, and a pitch-controllable UUV—and to an iterative testing process in which failures observed at sea are traced to a specific subsystem and removed by design before retest. Representative outcomes include UAV Tin-pickup success raised from near zero to about 80%, search-confirmation reliability improved from 12/20 to 20/20, aerial localization dispersion reduced from 0.57 m to 0.15 m, UUV pitch held near ±5°, and verified autonomous recovery after deliberate perception loss.

I. COMPETITION STRATEGY

A. Strategic Vision The 2026 Maritime RobotX Challenge places increased emphasis on autonomy and on collaborative behaviors across domains [1]. Every additional cooperative behavior, however, multiplies the number of interfaces that must be integrated and tested, and with a fixed number of preparation hours the binding constraint is not ideas but *testing time*. KMOU MACRO's strategic vision therefore treats each new capability as a claim on that budget and admits it to the competition configuration only once field testing shows it to be repeatable.

This vision is grounded in the team's own history. In 2024, our UAV crashed during Tin retrieval; post-analysis attributed the loss not to control software but to selecting motors without a thrust budget, so that the fully loaded vehicle flew near full throttle and could not be recovered once the link degraded. An early-2026 F550 re-test, even after conversion to a hexacopter, reproduced the same instability with the winch mounted. Two independent observations of the same root cause reframed our priority: *secure margin first (thrust, endurance, communication), and add function only on top of that margin*.

We compete as a three-domain SoS—Apex (USV), Windy (UAV), and Nautilus (UUV) (Fig. 1)—and attempt the Disruptive tier on all four tasks, with each task led by the domains that can uniquely supply the required capability (Table 1).

B. Complexity–Reliability Trade-offs We made three deliberate trade-offs, each judged by a measurement rather than by preference.

Margin over features. Rather than adding perception capability to a marginal airframe, we rebuilt the UAV from the payload up (Sec. II-D). The cost was half a season of feature development; the return



Figure 1: KMOU MACRO multi-domain platforms for the 2026 Maritime RobotX Challenge: Apex (USV, surface coordination), Windy (UAV, aerial perception and logistics), and Nautilus (UUV, underwater survey and interaction).

Table 1: Selected autonomy-challenge tasks and the rationale linking them to the SoS design.

Task	Target Tier	Key Autonomous Behavior	Lead Domains
1 Safe Passage	Disruptive	UAV judges the color/position of top-only LED buoys and relays them to the USV, which forms a live gate-to-gate passage	UAV + USV
2 Infrastructure Survey	Disruptive	USV deploys the UUV from its underside; the UUV surveys the underwater pipe by sonar, performs LED tagging, and reports to the USV	USV + UUV
3 Coordinated Logistics	Disruptive	USV relays the requested color; the UAV autonomously retrieves the matching Tin and delivers it to the designated color circle	USV + UAV
4 Dynamic Incident Response	Disruptive	On command, each platform suspends its task, transits to the designated coordinate, holds, and reports readiness	All (SoS layer)

was a platform whose pickup success rose from effectively 0% (F550, winch mounted) to about 80% over more than ten trials.

Repeatability over speed. The UAV's initial search accepted detections while moving and confirmed targets in only 12 of 20 randomized simulations. Restricting perception to a hover at each search cell raised this to 20/20 at the cost of a ∼35% increase in search time—a cost we accepted because a task scored on completion rewards repeatable detection over fast coverage.

Bounded dependency over full connectivity. Fully connecting three vehicles would create three inter-vehicle interfaces and triple the integration-test combinations. We instead keep the USV as the sole hub, maintaining only two links—UAV↔USV (wireless MAVLink) and UUV↔USV (tether)—so that a failure of one link cannot stall another domain.

C. System of Systems Mission Flow Collaboration is organized by sharing mission-level information and then letting each vehicle act with its own local autonomy, not by centralizing low-level control (Fig. 2).

In *Safe Passage*, the UAV supplies buoy semantics the surface cannot see; once the USV can observe the same buoys with LiDAR, the current gate is judged by fusing the UAV's semantic class with the USV's local geometry. Aerial observation thus serves early perception and planning while USV LiDAR serves local confirmation and navigation. In *Infrastructure Survey*, the USV provides transport and mission initiation while the UUV ex-

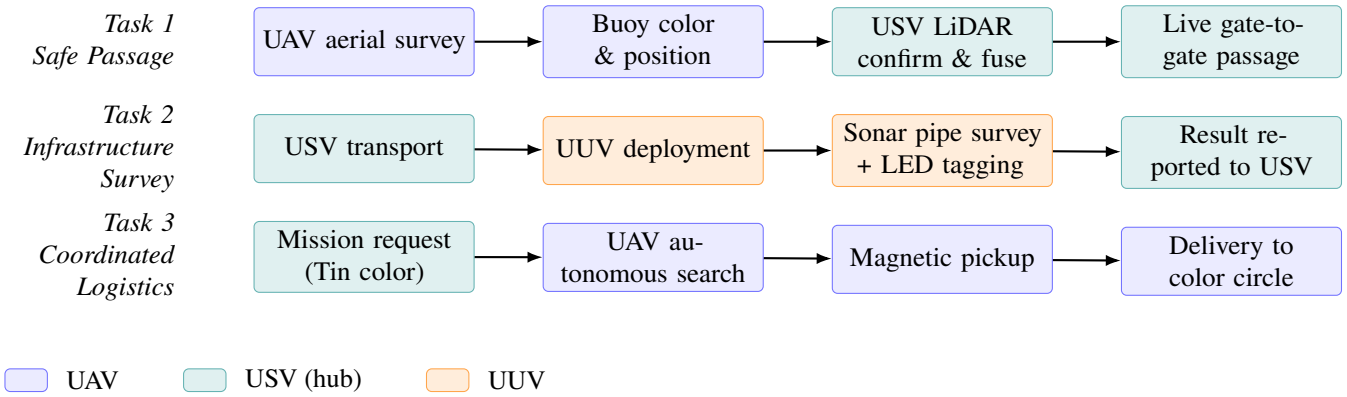


Figure 2: Collaborative mission flow and division of autonomy among the USV, UAV, and UUV.

ecutes the underwater task with local autonomy. In *Coordinated Logistics*, the global decision (which Tin color) is shared at the SoS level while the perception and physical execution stay inside the UAV. *Dynamic Incident Response* is handled in the mission-coordination layer as an SoS-level interruption rather than as vehicle-specific logic.

II. DESIGN STRATEGY

A. Systems Engineering Approach Requirements flow down from each task's failure conditions to a per-vehicle role, and every design change is driven by a limit observed in testing rather than by a specification improvement in isolation. Interfaces are defined once and shared by all layers as a fixed contract, so that a change in one algorithm cannot silently alter another vehicle's behavior. Verification follows a staged gate (Sec. III) in which a change must pass a lower-risk stage before it is promoted. Lessons from 2024—where VRX and Hardware-in-the-Loop Simulation (HILS) [2] caught communication and mission-logic faults before sea trials—were extended in 2026 from the USV to the UAV and UUV, each with a domain-appropriate simulator. The software toolchain that realizes these tasks is listed in Table 2.

B. System of Systems Architecture and Integration The SoS is organized in three tiers (Fig. 3): the competition network and Operator Control Station (OCS) ashore, the USV as mission-coordination and communication hub, and the UAV and UUV as locally autonomous vehicles. Every vehicle runs the same four-layer stack—mission decision, perception, control, and hardware—in its own ROS 2 domain, and only mission-level commands, targets, states, and results cross a vehicle boundary. Beyond modularity, this layering exists to localize a failure so that only the responsible layer is revised and

Table 2: Software toolchain across the System of Systems.

Function	Tools
Middleware / integration	ROS 2 with per-vehicle domain isolation
Flight & payload control	ArduPilot, MAVROS, Lua winch script
Onboard inference	YOLO on Hailo NPU (~20 fps) [4]; HSV/threshold
Underwater perception	U-Net [5], RANSAC [6], Bayesian mapping, threshold LED
Surface perception / fusion	LiDAR clustering with ICP registration [7]
Simulation	VRX/Gazebo (USV) [2], ArduPilot SITL (UAV), DAVE (UUV) [3]
Command & logging	Web GCS, RoboCommand client, full-flight rosbag

retested.

Upward integration. Toward the competition infrastructure the SoS presents a single point of contact. RoboCommand traffic arrives as MQTT/protobuf messages, and an OCS bridge translates it to and from ROS 2 topics; competition commands and task reports therefore look to the vehicle software like any other topic, and a protocol change is absorbed in the bridge rather than in three vehicles. The SoS mission coordinator on the USV owns the task sequence: it starts and stops vehicle-level tasks, merges each vehicle's state into the report sent ashore, and implements Dynamic Incident Response as a preemption of whichever task FSM is active, instead of duplicating that logic per vehicle.

Downward integration. The hub maintains exactly two vehicle links (Table 3). The UAV link is a CUAV P9 radio that connects the two vehicles directly, without passing through the ground station; mission data travel as compact TLV-encoded payloads inside MAVLink 2 `TUNNEL` messages, so a few bytes per message survive a low-rate radio that could not carry ROS 2 traffic. The SIYI HM30 link between the UAV and the ground serves the ground station and RC pilot and is kept separate from this path. On the UUV link, the tether carries commands and results while a separate steel wire takes the mechanical load. Each vehicle's mission FSM consumes these messages as inputs to its own decisions; the hub never commands another vehicle's actuators, which is what keeps a degraded link from becoming a loss of control.

Table 3: Hub interfaces and their mission-level content (↓ to vehicle, ↑ to hub/shore).

Link	Protocol and content
OCS–USV	Shore radio link. ↓ task start/stop, incident coordinate; ↑ SoS state, results
USV–UAV	CUAV P9 radio, MAVLink 2 `TUNNEL` with TLV payload. ↓ requested Tin color, suspend/go-to; ↑ buoy class and position, pickup/delivery state, readiness
USV–UUV	Tether. ↓ deploy/start, suspend; ↑ pipe-survey result, LED-tag report, state

C. Vehicle Subsystems Table 4 lists the configuration of each vehicle in the same layers as Fig. 3.

Apex (USV). Apex is a monohull designed and fabricated in-house, 1.78 m long and 0.67 m wide at about 58 kg. A Pixhawk 6X running ArduRover closes the inner loop and is commanded through MAVROS by an NVIDIA Jetson Thor mission computer, which hosts the SoS coordinator, surface perception, and guidance. Two azimuth pods, each a Blue Robotics T500 thruster with independent steering, provide surge, sway, and yaw. A Livox Avia LiDAR supplies buoy and dock geometry, complemented by onboard cameras, and a CUAV C-RTK 2HP GNSS receiver provides navigation. Mission equipment comprises the pan-tilt water-delivery nozzle with its IP camera and pump, the deck winch that manages the UUV tether, and the underbody profile that carries Nautilus. The status light is driven by an ArduPilot Lua script through a PWM output, so it shows the autopilot's actual arming state and mode even if the mission computer has failed.

Windy (UAV). Windy is a Tarot X6 hexacopter flown by a Pixhawk 6X running ArduCopter. Onboard YOLO inference on a Raspberry Pi with a Hailo NPU removes ground-station round-trip latency from the visual-servoing loop, and the winch is driven by a Lua script on the Pixhawk so that a companion-computer fault cannot command it.

Nautilus (UUV). Nautilus is a tethered Blue Robotics BlueROV2 in the Heavy configuration, whose eight T200 thrusters add active pitch control to the original six-thruster arrangement. A Sonoptix ECHO multibeam imaging sonar on a 35° mount is the primary sensor for pipe search and tracking, a camera serves the close-range LED interaction, and attitude comes from the IMU inside the Navigator flight controller. On an Intel NUC mini PC, sonar frames are segmented by a U-Net [5], the pipe is fitted as a line by RANSAC [6], and detections are accumulated in a Bayesian map; waypoints are generated from the nearest mapped segment, and the controller holds altitude, heading, and pitch so the pipe stays inside the sonar field of view. The same map is the recovery reference: on perception

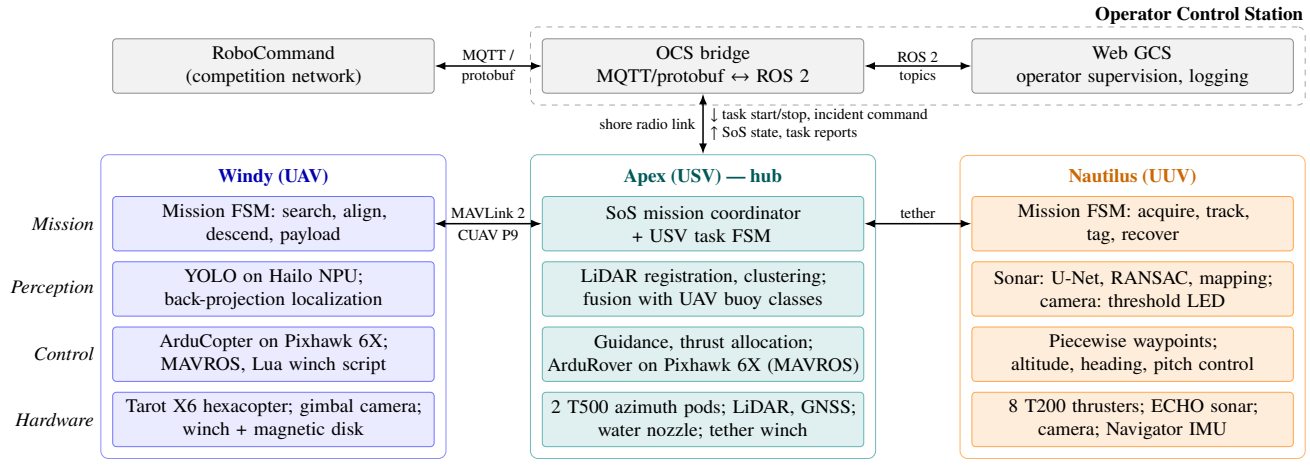


Figure 3: System-of-Systems architecture and its integration with the upper system. Every vehicle runs the same four-layer stack; only the mission layer communicates across vehicles, always through the USV hub, and the hub is the single point of contact with the OCS and RoboCommand.

loss the vehicle returns to the last valid mapped point and resumes tracking. Power comes from a 14.4 V, 18 Ah (263 Wh) Li-ion pack in a housing that is charged through an external port, so it is not opened for charging.

D. Mission-Critical Design Decisions A single criterion governs the major redesigns: *distinguish what software can compensate from the physical authority hardware must provide, and where the control margin itself is lacking, change the platform before complicating the algorithm.*

1) Mobility and Operating Margin USV lateral authority. We developed an azimuth thruster arrangement that gives the vessel pure sway, that is, lateral translation without yaw (Fig. 4). Two thrust inputs and two steering angles provide four inputs for three degrees of freedom, and a thrust-allocation layer maps the commanded surge, sway, and yaw onto them. A vectored four-thruster layout would give the same freedoms but raises part count and power draw and requires the hull to be redesigned; two steerable pods provide what docking demands while reusing the existing hull.

UAV payload margin. The compact F550 frame limits propeller size, so converting it to a hexacopter added little thrust margin. We therefore sized a new airframe from the full payload (winch, magnetic disk, gimbal, companion computer, Tin). The Tarot X6 takes off at 6.4 kg against the 7 kg

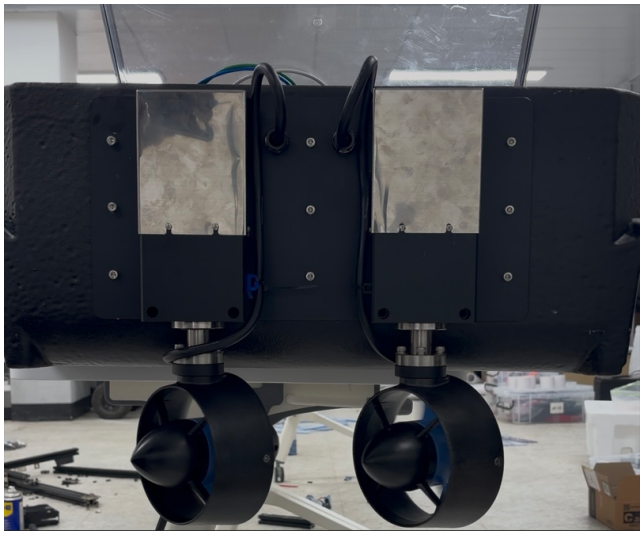


Figure 4: Two-pod azimuth thruster arrangement on the USV, providing pure sway for lane alignment during docking.

limit, a margin of $(7.0 - 6.4)/7.0 \approx 8.6\%$, with propulsion sized for a thrust-to-weight ratio of at least 2:1 so that hover throttle stays low enough to retain single-motor-out recovery.

UUV attitude authority. In the initial 6-thruster configuration, sea-state disturbance drove pitch motions that pushed the pipe out of the sonar field of view. We changed to an 8-thruster Heavy configuration with pitch control and re-verified sonar tracking; forward-motion pitch then stabilized, with its standard deviation falling from 6.9° to 1.4° and

Table 4: Vehicle system configuration.

	Apex (USV, hub)	Windy (UAV)	Nautilus (UUV)
Platform	In-house monohull, $1.78 \times 0.67 \times 0.42$ m (L×B×H), ≈58 kg	Tarot X6 hexacopter, 6.4 kg takeoff	Blue Robotics BlueROV2, Heavy configuration, tethered
Propulsion	2 azimuth pods (Blue Robotics T500), thrust + steering each	$6 \times$ 5008 KV340 motors	$8 \times$ Blue Robotics T200 thrusters
Computing	Pixhawk 6X (ArduRover); NVIDIA Jetson Thor	Pixhawk 6X (ArduCopter, Lua winch script); Raspberry Pi + Hailo NPU	Navigator flight controller; Intel NUC mini PC
Sensors	Livox Avia LiDAR, cameras, CUAV C-RTK 2HP GNSS	Gimbal camera (1280×720), GNSS	Sonoptix ECHO multibeam imaging sonar at 35°, camera, Navigator internal IMU
Mission payload	Pan-tilt water nozzle with IP camera and pump; tether winch; UUV underbody profile	Winch + magnetic disk	Camera-guided close-range LED tagging
Links	Shore radio link; CUAV P9 to UAV; UUV tether	CUAV P9 direct to USV (MAVLink 2); SIYI HM30 to ground station and RC	Tether to USV deck winch
Power	6S 18 Ah	6S 18 Ah	Li-ion 14.4 V / 18 Ah (263 Wh), external charging

99% of samples within ±5° (Fig. 8c). A sonar mounting-angle study from 15° to 40° at fixed altitude found the most stable detection at a 35° mount with a +10° pitch.

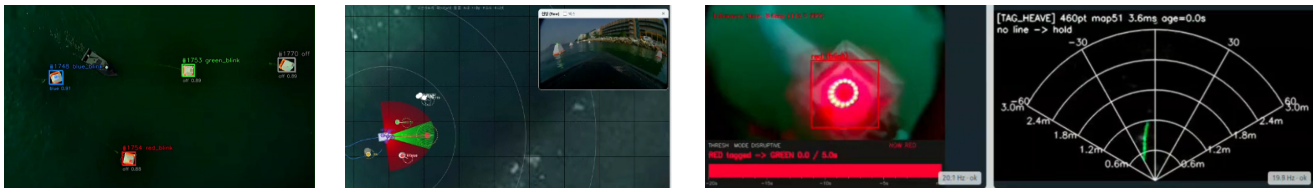
2) Perception under Environmental Uncertainty Perception conditions change continuously with illumination, wave reflection, turbidity, motion, and range, so each sensor takes a role where it is most valid and uncertain observations do not translate directly into action.

Measure the camera, don't model the error. Aerial positions are obtained by back-projecting tracked pixels through the gimbal camera's measured intrinsics and distortion model, gimbal attitude, and ground altitude. Replacing the nominal pinhole model with the measured calibration reduced the median repeat-observation dispersion of the same buoy from 0.57 m to 0.15 m across 27 field tracks.

Derive the search from the sensor. An operator marks four corners; the FSM fits the minimum rectangle and divides it by the measured ground footprint (17.62×9.37 m at 10 m altitude), so a 60× 40 m course with 1 m overlap yields $\lceil 60/16.62 \rceil \times \lceil 40/8.37 \rceil = 4 \times 5 = 20$ cells, re-computed if altitude changes. Perception runs while hovering at each cell, with transit limited to 2 m/s, which raised confirmation from 12/20 to 20/20 (mean position error 0.22 m, max 0.37 m).

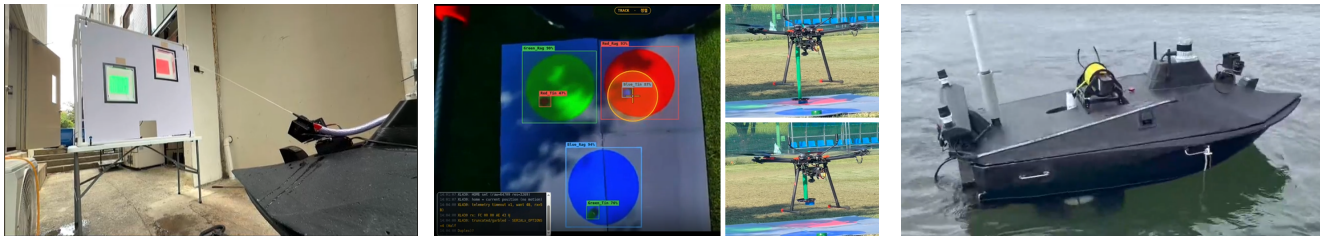
Split semantics from geometry on the surface. The Safe Passage buoy LEDs are visible only from above, so the USV does not try to classify them. Its LiDAR returns are registered by ICP [7] and clustered into a local map, and each cluster is associated with the UAV-reported buoy positions to obtain its color class; the gate is thus formed from geometry the USV is observing at that moment, not from a pre-surveyed route.

Separate the underwater sensing problems. Pipe search/tracking uses sonar, which is robust to visi-



(a) UAV **(b)** USV **(c)** UUV

Figure 5: Complementary perception across domains: (a) UAV aerial buoy detection with tracked IDs and blink-state classification, (b) USV surface map with sensor coverage sectors and detected buoys, alongside the raw camera view, and (c) UUV threshold-based LED tagging (left) and sonar pipe detection in the polar view (right).



(a) Water delivery **(b)** UAV Tin pickup **(c)** USV–UUV integration

Figure 6: Mission-critical physical interactions: (a) water delivery from the shared nozzle–camera pan-tilt jig, (b) UAV magnetic Tin pickup—onboard detection and alignment (left), disk contact and lift with a pre-lowered winch cable (right), and (c) USV underway with the UUV mounted beneath the hull (submerged), held by the underbody profile and steel wire, with the tether winch on deck.

bility; distant bends that distorted a global line fit were removed by generating waypoints from the nearest pipe segment (Piecewise). LED interaction needs color, so it uses the camera but with threshold processing rather than a learned model—chosen not only to cut computation but so the threshold can be re-tuned on site through a GUI without collecting a dataset and retraining. Fig. 5 shows the complementary perception across domains.

3) Physical Interaction and Mission Execution Physical interactions add mechanical tolerance, reduced disturbance exposure, and fault containment to control accuracy. In docking, the vehicle holds heading normal to the wall, aligns to the lane centerline with pure sway, and only then enters on surge, so diagonal entry is excluded by geometry rather than corrected afterward. For water delivery, nozzle and camera share one two-axis pan-tilt jig so the measured angular error is the servo command; the initial USB camera was replaced by a configurable IP camera to match course lighting. For Tin pickup, a winch and magnetic disk replace a gripper, removing jaw failure modes; the plate was widened into a disk so horizontal offset just before contact is absorbed as tolerance, and most of the cable is pre-lowered so winch exposure to wind is minimized. UUV LED tagging is a close-range contact task, so Heavy-configuration attitude control and field-adjustable perception are used together. The USV–UUV interface balances UUV stability against USV maneuverability: instead of rigid coupling, an underbody profile matched to the UUV width constrains heading while a steel wire relieves tether load (Fig. 6).

E. Key Design Trade Studies Table 5 records the principal alternatives considered and the reason each decision was made.

III. TESTING STRATEGY

A. Verification Philosophy Verification climbs a staged gate (Fig. 7)—simulation/recorded data → controlled test → field test → integrated mission test—and a change that fails a stage is not promoted. Because waves, current, sunlight, turbidity, and vehicle interaction are hard to reproduce, simulation success is never the final criterion; the pass condi-

Table 5: Key design trade studies (chosen option in bold).

Decision	Alternatives	Basis
USV lateral DOF	twin-screw / vectored-4 / **2-pod azimuth**	pure sway while reusing the hull
UAV airframe	F550 quad / F550 hexa / **Tarot X6 hexa**	payload margin, motor-out recovery
UAV capture	gripper / **winch + magnetic disk**	no jaw failure, offset tolerance
UUV thruster layout	6-thruster / **8-thruster Heavy**	pitch authority keeps the pipe in the sonar field of view
UUV LED perception	YOLO learned / **threshold + GUI**	low compute, field-adjustable
Coordination	fully connected / **USV hub**	fewer interfaces, fault isolation

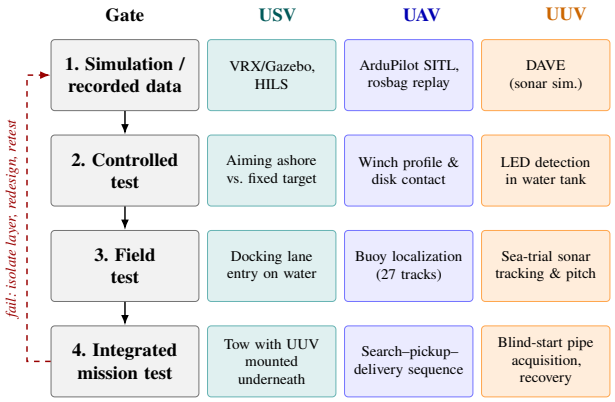


Figure 7: Progressive verification from simulation and recorded data to integrated field validation, with per-vehicle tests at each gate (USV: VRX/HILS; UAV: SITL / rosbag replay; UUV: DAVE / sea-trial sonar). A change is promoted only after passing the lower gate; a failure is traced to its layer and retested at the same gate after redesign.

tion is repeatable execution in the real environment. Crucially, we record not only successes but failure causes, separate them across the perception, planning, control, mechanical, and communication layers, and retest the redesign under the same conditions.

B. Simulation and Software-in-the-Loop USV task logic and path following are verified in VRX/Gazebo [2]; UAV mission FSM and state transitions in ArduPilot SITL; and UUV pipe-tracking control in the sonar-capable DAVE simulator [3]. Dynamics-independent pure functions—rectangle fitting, grid generation, route planning—are unit-tested apart from the ROS runtime, with the path planner exercised on 3,000 randomized inputs for waypoint count, boundary conditions, and path validity.

C. Component and Laboratory Testing Individual components are verified before integration: the aiming subsystem (camera, pose estimation, pan-tilt loop, pump) was brought up ashore against a fixed target and used to measure the distance-to-tilt offset; the winch descent profile and magnetic-disk contact were checked in isolation; and camera-based LED detection and sequence logic were validated in a controlled water tank, where they operated without issue before facing field lighting.

D. Subsystem and Field Testing Subsystems are then exercised on race-like geometry with external disturbances. Sea trials revealed model detection failures and sonar FOV departure not seen in simulation or tank, which became the basis for the Heavy-configuration and Piecewise-waypoint changes. All flights are logged to rosbag so a perception change can be regression-tested on the same input without a new flight. The overall verification status is summarized in Table 6.

E. Test-Driven Design Changes Testing determined the next design requirement rather than merely grading a finished one (Table 7). Each change listed there was an engineering response to an observed failure mode. Recovery was verified not only nominally but by pulling the tether hard twice to force perception loss, after which the UUV returned to the last valid mapping point and resumed tracking. A safety failure—battery flooding through an open housing vent—was removed at the source by a housing that charges externally without

Table 6: Verification matrix (representative results).

Capability	Domain	Test Level	Metric / Result
Buoy localization	UAV	Field, 27 tracks	dispersion 0.57 → 0.15 m
Search confirmation	UAV	Randomized simulation (×20)	12/20 → 20/20
Tin pickup	UAV	Ground/field (>10 trials)	≈80% success
Visual alignment	UAV	Field	18 px (tolerance 70 px)
Pipe acquisition	UUV	DAVE → sea	verified from blind start
Attitude	UUV	Sea	pitch ≈ ±5°
Recovery	UUV	Sea, induced perception loss	re-acquisition verified
Docking	USV	Water	lane entry via azimuth sway
USV–UUV tow	SoS	Sea	stable during USV mission

opening. Representative quantified improvements are shown in Fig. 8.

F. Integrated Validation and Remaining Work

Because subsystem success does not guarantee mission success, the final stage verifies end-to-end sequences including inter-vehicle communication, mission transition, and physical interaction. The UAV has completed the full autonomous search–pickup–delivery sequence without pre-loading; the UUV has acquired and tracked the pipe by sonar from a camera-blind start; and USV–UUV integration has been exercised with the UUV mounted underneath during other USV missions. Two Safe-Passage items found at sea—low red-class confidence and an anomalous back-projection altitude input—are being corrected by augmented-data retraining and by switching the altitude input to raw GPS, respectively, and precise LED tagging under strong disturbance remains a controller-tuning target. Each will be confirmed only after passing the same retest gate, and the results recorded in the final integrated-validation table.

IV. CONCLUSION

The competition, design, and testing strategies form one coherent approach. The competition strategy defines success as the reliability of a USV-centered SoS and sets three principles: prefer live information over precomputed information, prioritize physical margin and repeatability over feature count, and add only the degrees of freedom each task needs. The design strategy realizes these as a USV-hub architecture with distributed autonomy, margin-securing platform redesigns justified by explicit calculation, and perception and interaction designs matched to real conditions. The testing strategy closes the loop by reproducing failures, isolating their cause by layer, and removing it by design before retest. The measured outcomes—≈80% pickup, 20/20 search confirmation, 0.15 m localization, ±5° pitch, and verified recovery—indicate the operational strength this approach is expected to bring to Marina Bay: a bounded set of cooperative behaviors that can be completed repeatably.

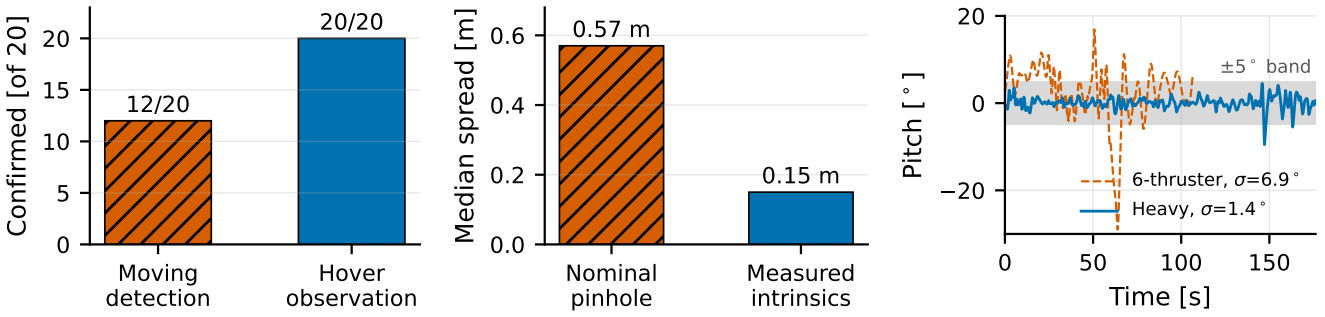
ACKNOWLEDGEMENTS

The authors thank Prof. Joohyun Woo and the MACRO Laboratory at Korea Maritime & Ocean University for research supervision, laboratory facilities, and technical guidance throughout the design and sea-trial campaign, and the team's members for hardware fabrication, software development, and field-test operations. We gratefully acknowledge Avikus, LIG D&A, the Korea Institute of Ocean Science and Technology (KIOST), and the Korea Research Institute of Ships and Ocean Engineering (KRISO) for their financial support, which made the development and field validation of the team's autonomous maritime platforms possible.

REFERENCES

[1] RoboNation, *Maritime RobotX Challenge 2026 Team Handbook*, Aug. 7, 2026.

[2] B. Bingham *et al.*, "Toward maritime robotic



(a) UAV search confirmation **(b)** UAV buoy localization **(c)** UUV pitch

Figure 8: Representative test-driven improvements: (a) UAV search confirmation in 20 randomized simulations, (b) median repeat-observation dispersion of the same buoy over 27 field tracks, and (c) UUV pitch at sea before (6-thruster, 107 s at 20 Hz) and after (Heavy 8-thruster, 176 s at 5 Hz) the reconfiguration; the shaded band marks ±5°. The standard deviation fell from 6.9° to 1.4°, and 99.1% of post-change samples lie within the band.

Table 7: Test-driven design evolution across the three domains.

System	Initial Approach	Test Observation	Design Change	Verification
USV Safe Passage	Pre-surveyed route	Position/state uncertainty	Live UAV + LiDAR navigation	Field test
USV Docking	Fixed-shaft propulsion	Diagonal approach	Azimuth + sway alignment	Water test
UAV Platform	F550 (quad → hexa)	Payload instability	Tarot X6 frame	Pickup ≈80%
UAV Search	Moving detection	12/20 confirmation	Hover observation	20/20
UAV Localization	Nominal camera model	Large position spread	Measured calibration	0.57 → 0.15 m
UUV Platform	Limited pitch control	Sonar FOV instability	Heavy / 8-thruster	Pitch ≈ ±5°
UUV Pipe Tracking	Global line interpretation	Distant-bend interference	Local Piecewise waypoint	Sea retest
UUV LED Perception	YOLO sequence inference	Compute/environment sensitivity	Adjustable threshold	Field verified
USV–UUV Interface	Tether-only	UUV attitude instability	Underbody profile	Integrated sea test

simulation in Gazebo," in *Proc. MTS/IEEE OCEANS*, Seattle, WA, USA, 2019, pp. 1–10.

[3] M. M. Zhang *et al.*, "DAVE Aquatic Virtual Environment: Toward a general underwater robotics simulator," in *Proc. IEEE/OES Autonomous Underwater Vehicles Symp. (AUV)*, 2022, pp. 1–8.

[4] J. Redmon, S. Divvala, R. Girshick, and A. Farhadi, "You Only Look Once: Unified, real-time object detection," in *Proc. IEEE Conf. Computer Vision and Pattern Recognition (CVPR)*, 2016, pp. 779–788.

[5] O. Ronneberger, P. Fischer, and T. Brox, "U-Net: Convolutional networks for biomedical image segmentation," in *Proc. Med. Image Comput. Comput.-Assist. Interv. (MICCAI)*, 2015, pp. 234–241.

[6] M. A. Fischler and R. C. Bolles, "Random sam-

ple consensus: A paradigm for model fitting with applications to image analysis and automated cartography," *Commun. ACM*, vol. 24, no. 6, pp. 381–395, 1981.

[7] P. J. Besl and N. D. McKay, "A method for registration of 3-D shapes," *IEEE Trans. Pattern Anal. Mach. Intell.*, vol. 14, no. 2, pp. 239–256, 1992.